

A HIGH CONTRAST IMAGING SURVEY OF SIM LITE PLANET SEARCH TARGETS

ANGELE M. TANNER¹, CHRISTOPHER R. GELINO², NICHOLAS M. LAW³

Draft version October 7, 2018

ABSTRACT

With the development of extreme high contrast ground-based adaptive optics instruments and space missions aimed at detecting and characterizing Jupiter- and terrestrial-mass planets, it is critical that each target star be thoroughly vetted to determine whether it is a viable target given both the instrumental design and scientific goals of the program. With this in mind, we have conducted a high contrast imaging survey of mature AFGKM stars with the PALAO/PHARO instrument on the Palomar 200 inch telescope. The survey reached sensitivities sufficient to detect brown dwarf companions at separations of > 50 AU. The results of this survey will be utilized both by future direct imaging projects such as GPI, SPHERE and P1640 and indirect detection missions such as SIM Lite. Out of 84 targets, all but one have no close-in (0.45 - $1''$) companions and 64 (76%) have no stars at all within the $25''$ field-of-view. The sensitivity contrasts in the K_s passband ranged from 4.5 to 10 for this set of observations. These stars were selected as the best nearby targets for habitable planet searches owing to their long-lived habitable zones (> 1 billion years). We report two stars, GJ 454 and GJ 1020, with previously unpublished proper motion companions. In both cases, the companions are stellar in nature and are most likely M dwarfs based on their absolute magnitudes and colors. Based on our mass sensitivities and level of completeness, we can place an upper limit of $\sim 17\%$ on the presence of brown dwarf companions with masses $> 40 M_J$ at separations of > 1 arcsecond. We also discuss the importance of including statistics on those stars with no detected companions in their field of view for the sake of future companion searches and an overall understanding of the population of low-mass objects around nearby stars.

1. INTRODUCTION

For the last decade, planet search efforts around nearby stars have been led by radial velocity surveys which are sensitive to Jupiter mass planets with close-in (< 5 AU) orbits (Butler et al. 2006). High contrast imaging surveys have recently culminated with the direct detection of Jupiter-mass planets at wider separations (> 20 AU, Marois et al. 2008; Kalas et al. 2008). While the radial velocity surveys are approaching sensitivities capable of detecting hot super-Earth mass planets around solar-mass stars and even habitable terrestrial-mass planets around some low-mass stars, Earth analogs remain out of reach due to intrinsic stellar jitter. SIM Lite (formally called SIM PlanetQuest, Unwin et al. 2008) will be the first instrument capable of detecting Earth analogs in the habitable zone of nearby stars. SIM Lite is a planned space-based interferometer with two 50 cm telescopes separated by 6 meters. It is capable of achieving a single measurement positional accuracy of $1 \mu\text{as}$, enough to detect terrestrial planets in the habitable zone of nearby solar-type stars.

There are two SIM Key projects chosen to conduct surveys capable of detecting terrestrial-mass planets around nearby main sequence stars - Discovery of Planetary Systems (Geoff Marcy, PI) and the Extrasolar Planets Interferometric Survey (EPICs, Mike Shao, PI). These projects will carry out an astrometric search for rocky

planets around ~ 200 stars located within 30 pc of the Sun.

There are many precursor programs currently being conducted to characterize and vet all potential targets for all the SIM Key projects (Unwin et al. 2008). These programs include radial velocity studies of the reference stars utilized in the narrow-angle observations, accurate spectral type determinations through optical spectroscopy, and photometry studies of the stars in the young star planet search program. Some of these programs have resulted in planet detections themselves (Niedzielski et al. 2007) or data that can be applied to upcoming planet surveys (Tanner et al. 2007). Here, we present the results of a companion survey of stars included in both of the terrestrial planet SIM Lite surveys. The observational goal of this companion survey is to identify bright, nearby companions to the target stars. A companion with $\Delta V < 4$ and within $1''$ can bias the position of the photocenter of the star, thus reducing the astrometric accuracy. While this survey was designed as a precursor program for SIM Lite, the observations presented here also serve as reconnaissance data for upcoming high contrast imaging surveys such as the Gemini Planet Imager (GPI) (Macintosh et al. 2006), the VLT SPHERE coronagraph (Beuzit et al. 2008) and P1640, the recently commissioned Lyot AO coronagraph on the Palomar 200 inch telescope (Hinkley et al. 2008). As a result of the high contrast images collected for this survey, for most of the stars in the sample, we are sensitive to brown dwarf mass objects at separations of > 50 AU. Because this program is sensitive to brown dwarf companions at wide separations, the results serve as an additional probe of the brown dwarf desert.

Section 2 describes the criteria by which we created the

¹ Georgia State University, Department of Astronomy, One Park Place, Atlanta, GA, angelle.tanner@gmail.com

² Infrared Processing and Analysis Center, 770 S. Wilson Ave. Pasadena, CA 91125

³ Dunlap Institute for Astronomy and Astrophysics, University of Toronto, 50 St. George Street, Toronto Ontario, Canada, M5S 3H4

sample for the survey, § 3 details our observations, § 4 describes the data reduction and analysis, § 5 summarizes the results of the survey and our achieved sensitivities and in § 6 we compare our results to previous surveys and discuss the importance of publishing non-detections.

2. SAMPLE SELECTION

The two SIM Lite terrestrial planet search programs coordinated their target selection so as to create unique lists for each team. Since one of the projects is primarily interested in finding terrestrial planets in the habitable zone (“Extrasolar Planets Interferometric Survey (EPIcS)”, Shao, PI) and the other is aimed at detecting all planets around stars within 8 pc (“Discovery of Planetary Systems”, Marcy, PI), it was not difficult to agree on the two samples.⁴ Target stars were selected based on spectral type, heliocentric distance, brightness, companion separation (if applicable), habitable zone location, and the orbital period at the habitable zone.

Since these lists were created, the EPIcS program completed a study on how to further optimize the list. An additional sample list of 240 stars has been created for the purpose of performing Monte Carlo simulations to predict the potential yield of a SIM Lite terrestrial-planet search program (Catanzarite et al. 2006). This SIM-optimized target list is derived from an initial list of 2350 stars taken from the Hipparcos catalog, with distances of less than 30 pc (Turnbull & Tarter 2003). They excluded stars with luminosity greater than 25 times solar, thereby eliminating giants from our sample. To eliminate the possibility of fringe contamination from a binary companion, we applied the following: stars with a known companion closer than $0.4''$ and $\Delta V < 4$ were excluded. If the target-star candidate had a wide binary companion that was separated by more than $1.5''$, the companion was added to the list of target-star candidates. Further improvements on the target ranking will include considerations of stellar metallicity and the number and orientation of the reference stars with respect to the target. In the end, these stars will represent the best targets for a micro-arcsecond astrometric planet search.

After two years of observations, we have collected observations for a subset of 84 nearby, main sequence (V) stars taken from both the original EPIcS sample and the one created for Catanzarite et al. (2006). The properties of each of the stars in the sample are given in Table 2. The stars in our sample have distances of 3.5-30 pc, spectral types of M4-A3V and V magnitudes of 0.77-11.35. Most if not all of the stars in the sample are mature stars with ages of 1-10 Gyr. We made sure not to observe those stars with published AO coronagraphic or Hubble Space telescope observations (Carson et al. 2007; Lowrance et al. 2005; Metchev et al. 2005).

3. OBSERVATIONS

Observations were obtained with the Palomar Observatory Hale 5m Telescope using the PHARO near-IR camera (Hayward et al. 2001) behind the PALAO adaptive optics (AO) system (Troy et al. 2000). Observing dates and sky conditions are given in Table 2. We used a 25 mas/pixel scale camera ($25''$ field of view) and the $0.45''$

radius occulting spot. Each star was observed in the K_s filter ($2.16 \mu\text{m}$) with integration times of 1–30 seconds, depending on the brightness of the star. Stacks of 20–100 short exposure images were collected for each star resulting in effective integration times of 100–1200 seconds⁵. Stacks of sky images were taken adjacent to each set of target images by offsetting $30''$ from the target in the four cardinal directions and turning off the AO system. For flux calibration, observations of the target stars were taken by inserting the neutral density filter, offsetting the star from the coronagraph and placing it in a five point dither pattern to allow for adequate sky subtraction⁶. These offset images allowed us to determine that the FWHM of the AO corrected observations varied from 0.2 to $1.3''$ with Strehl ratios of 0.20–0.74. The seeing quality varies considerably for the different observing runs, from “good” ($0.5''$) to bad ($>3''$) based on the FWHM of the point spread function (PSF) with no AO correction (see Table 3). The variable seeing affected our ability to achieve uniform sensitivities for all the target stars in the survey.

To aid in the suppression of speckle noise, we observed a set of PSF stars in conjunction with about half of our targets. The PSF stars were selected to have similar colors (i.e. spectral types), brightness, and airmasses as the targets so as to produce a speckle pattern as close as possible to the science targets. Finally, sets of known binary stars with high quality orbital solutions were also observed during the 2005 November and 2004 October runs to provide an accurate determination of the plate scale and image orientation. During the observation, each binary was placed in multiple positions over the field of view of the camera. In order to observe as many targets as possible while also reaching image sensitivities necessary to detect brown dwarf companions, our observing goal was to complete all observations associated with each target within an half an hour.

4. DATA REDUCTION AND ANALYSIS

The individual AO images were sky-subtracted, flat-fielded and corrected for bad-pixels with the final image created from the median of the stack of reduced individual images. For those images with additional stars visible in the field of view, we used them to determine the offset of each image in the stack with respect to a reference image and shifted them accordingly prior to taking the median of the stack. This helped mitigate smearing from movement of the field during the observations due to telescope flexure or small losses in telescope tracking. A subset of the target images have corresponding observations of PSF stars with similar brightness and color. The relative positions of the target and PSF star were estimated using the Poisson spot present in the middle of the coronagraphic spot. As with previous studies (Metchev et al. 2004; Tanner et al. 2007) we are able to

⁵ Since the original SIM Lite Palomar survey started in 2004 was meant as a snap-shot program intended to look for close, stellar binaries, a subset of the coronagraphic observations were performed with a neutral density filter which reduced the effective integration times by a factor of 100. In most cases, those stars were reobserved without the neutral density filter to bring the effective integration times up to the level of the rest of the survey targets.

⁶ Flux calibration images were not collected during the June 2004 observing run.

⁴ The highest priority members of the combined target list are listed at <http://www.physics.sfsu.edu/~chris/SIM/t1.html>

register the star positions to 0.7 pixels using the centroid position of the spot (Tanner et al. 2007). The scaling for the PSF is the multiplicative factor which minimizes the residuals remaining after the subtraction. Comparisons of the standard deviations of the speckle noise of the stars before and after PSF subtraction suggest that the subtraction reduced the noise within the halo by $\sim 25\%$. Figure 1 shows the difference image of GL 876 and its PSF star HD 216789.

The coronagraphic images were flux calibrated using the images taken with the primary star off-set from the coronagraph while accounting for a difference in integration time and the well-defined neutral density filter used for the off-spot images (Metchev et al. 2004). The magnitudes for both the primary stars in the off-spot images and the companions in the coronagraphic images are estimated from aperture photometry with an aperture of $0.8''$ and sky annulus of $1.-1.25''$. The K_s band magnitudes of the primaries were taken from the Two Micron All-Sky Survey (Cutri et al. 2006). The uncertainties for the photometry were estimated from the errors given for the 2MASS magnitude and an assumption of a 5% calibration error determined by comparing the photometry of the companion to GJ 105a to published values (Golimowski et al. 2000).

The images of the calibration binaries were reduced in the standard manner. For the 2004 data, we assume a plate scale of 25.11 ± 0.04 mas pixel $^{-1}$ estimated from the known orbital solutions of three different binary stars (WDS 09006+4147, WDS 18055+0230, WDS 20467+1607) that were observed very close to our October observations using the same instrument (Oct 4-5, 2004, Metchev 2005, see their Table 4.1). For the 2005 data we estimate a plate scale of 25.21 ± 0.36 mas pixel $^{-1}$ using the average and standard deviation of the measured pixel separation of one binary (WDS 09006+4147, Hartkopf et al. 2006) compared to its predicted orbital separation in arcseconds. This binary, which was observed in November 2005, was placed in multiple positions across the field of view after correction for the known distortion in the camera.

A thorough visual inspection of both the median-averaged, coronagraphic images and the difference images between the targets and the PSF identified all stars in the $25''$ field of view. Those target stars with no additional stars visible in the field-of-view are listed in Table 4 while the companion candidates identified in these images are listed in Table 5 along with their distance from the target star, position angle and magnitude difference compared to the primary when available. To accurately determine the position of the star behind the coronagraphic spot, we utilized the static waffle pattern which has a distinct set of four speckles framing the PSF (see Figure 2). As determined in Tanner et al. (2007), by using the centroid position of each of the four spots in the waffle pattern, we can use the intersection of the lines crisscrossing the pattern to determine the star's position to 2.3 pixels. This positional accuracy and the error in the plate scale are then propagated when determining the uncertainties for the offset and position angle.

4.1. Common Proper Motion Determination

For thirteen of the stars with companion candidates, we collected second epoch observations at least a year

later during AO observing runs dedicated for other projects. The additional image allows us to determine whether the companion is bound to the star through their common proper motion. This positional accuracies given in Table 5 are sufficient to conclude whether the companion candidates are bound to their stars given the high proper motions (> 100 mas/yr) of all the stars in the sample and the minimum of a full year between observations. In most cases, simply blinking between the images shows the movement of the background star once the target star is held fixed. We determined the separation and position angles of the candidates in both images and compared them to what would be expected given the star's proper motion. After this analysis, we find two stars with confirmed common proper motion companions - GJ 454 and GJ 1020. The companions to these stars are new detections having not been mentioned in previous publications.

Figure 3 plots the offset in RA and Dec between GL 454 and its companion $1''$ away and Table 6 lists the astrometry. The solid line denotes the expected motion of the companion if it were a stationary background object. The fact that the offset of the companion star estimated for two different epochs does not change significantly given the associated errors (10-30 mas), confirms this object as a bona fide companion. Additional observations of GJ 454 at $1.25 \mu\text{m}$ where made with the same instrument during the June 2004 run and were reduced in the same way as the K_s data. Given the K_s and J magnitudes of the companion ($K_s=7.75$ and $J=9.07$) and the distance to the star (12.91 pc), it is most likely an M3 dwarf (Baraffe & Chabrier 1996). Despite its proximity to GJ 454, its relative brightness, $\Delta K_s > 6$, it should not pose a problem for SIM Lite. Figure 3 also shows the astrometry for the companion to GJ 1020, which was originally observed as a PSF star to GJ 10. This confirmed proper motion companion has a K_s magnitude of 10.4. With an absolute K magnitude of > 10 , this companion is most likely a low-mass star.

For some of the targets with no second epoch observations in our survey, we utilized images from the HST⁷, ESO⁸ and Gemini⁹ archives. We were able to use these archive data sets to confirm that companion candidates around GJ 726, GJ 722 and GJ 892 are background stars. There are 17 companion candidates that remain unconfirmed (see Table 5).

5. RESULTS

Out of 84 stars, we found two unpublished common proper motion companions to GJ 454 and GJ 1020, neither of which will cause problems for SIM Lite observations since it is much fainter than the target star. None of the companions have absolute magnitudes or colors consistent with brown dwarfs. This is not unexpected given the observed paucity of brown dwarf companions to solar mass main sequence stars (McCarthy & Zuckerman 2004; Butler et al. 2006).

5.1. Image Sensitivities

⁷ <http://archive.stsci.edu/hst/>

⁸ <http://archive.eso.org/cms/user-portal>

⁹ <http://www1.cadc-ccda.hia-ihh.nrc-cnrc.gc.ca/gsa/>

To estimate the sensitivities of all of our target fields as a function of distance from the star, we employ “PSF planting” in which a PSF corresponding to an object of known brightness is inserted into the image. The PSF extracted from the off-spot, flux-calibration image of each target is sky subtracted, normalized, multiplied by an array of contrast values ($\Delta K_s=7.7-15.1$ mags) and placed at a range (0-10'') of distances from the target at random position angles. We completed 10^4 iterations of the PSF planting algorithm to fill out the parameter space of contrast and distance from the primary star. We make sure that the same number of planted PSFs occur in each radius bin. To determine whether the planted star is detected, the image is cross-correlated with a flux normalized PSF. For each distance bin we estimate the minimum PSF intensity for which at least 90% of the fake sources had a correlation value of 0.75 or higher. This correlation value was determined by visually inspecting an image with inserted scaled PSFs. Previous studies have shown that the eye is often the best natural detector when determining the presence of a faint star in an image (Metchev et al. 2005).

The intensities are converted into magnitudes using the flux calibration from the off-spot image and the 2MASS K_s magnitude of the star. Figure 4 plots the largest K_s magnitude difference between the target star and planted PSF as a function of distance from the star for all targets with calibration data.

Table 7 lists the values of the faintest detectable K_s magnitudes at 0.5, 1, 2, and 5 arcseconds. We were able to detect sources with a magnitude contrast of $\Delta K_S \sim 4-6.5$ mag at 0.5'', $\Delta K_S \sim 5.5-8$ mag at 2'' and $\Delta K_S \sim 6.5-9.5$ at 5'' with $\sim 90\%$ completeness. The range of image contrasts is due primarily to variations in seeing conditions throughout the night. Unfortunately, the brightest objects suffer from two additional components of degradation in image sensitivity: 1) a smudge in the optics which creates a long streak across the spot at a position angle of 45 degrees, and 2) a thick, off-set ring due to a reflection off the array, entrance windows, or the coronagraphic slide which is illuminating the lyot stop (see Figure 5). These image artifacts reduce the sensitivity in these areas of the image by 15-20%.

5.2. Mass Sensitivities

By assuming a set of values relating the absolute magnitude of any brown dwarf companion to its mass and age based on theoretical evolution models (Burrows et al. 1997; Baraffe et al. 2003), we can estimate an lower limit to the mass sensitivity around those target stars with flux calibrations. Figure 6 plots the lower limits of the mass sensitivity at a separation of 1'' from each star as a function of separation in AU based on its Hipparcos distance. The upper limits assume both 1 Gyr (crosses) and 5 Gyr (asteriks) ages for the primary star. This plot shows that most of our observations are reaching into the brown dwarf regime ($\sim 75 M_J$) at separations of 1'' and beyond.

6. DISCUSSION

6.1. How does this survey compare with previous work?

There have been a few high contrast surveys consisting of similar samples of nearby, mature stars. Of those,

the most notable include McCarthy & Zuckerman (2004), a large non-AO coronagraphic survey of a couple hundred nearby, mature stars from which the “brown dwarf desert” was first posited at large (>100 AU) separations. Soon after this survey suggested that the percentage of mature stars with wide brown dwarf companions was comparable to the numbers determined from the RV surveys, $\sim 1\%$, additional coronagraphic AO surveys of similar targets suggested that this value is larger (3-10%) depending on the age of the targets and assuming non-circular orbits (Carson et al. 2006; Lowrance et al. 2005; Metchev et al. 2009). Based our mass sensitivities and level of completeness, at a separation of one arcsecond ($>5-60$ AU), we can place a 3σ upper limit of 17% on brown dwarf companions with masses down to $40 M_J$ at an age of 1 Gyr.

This survey presented here increases the sample of nearby, mature (>1 Gyr) stars with high contrast AO observations by over 50% when considering the “field” surveys listed in the table from Metchev et al. (2009). However, since the survey was originally designed as a precursor program to look for stellar companions to SIM Lite targets, our sample is not complete in a way that would allow us to provide improved limits on the brown dwarf companion fraction for the separations probed. However, these observations will be useful to future imaging surveys like GPI and SPHERE which are expected to be sensitive to planetary-mass objects as well as brown dwarfs.

6.2. The Value of publishing non-detections

With projects like GPI, SPHERE and SIM Lite being developed to focus almost primarily on the detection of exoplanets, it has become necessary to compile samples of targets which are going to yield the largest number of detections given the strengths and weaknesses of the instruments. Therefore, many years before these projects see first light, much effort is devoted to target selection, verification and precursor observations (i.e. Tanner et al. 2007; Carson et al. 2007). As a part of these precursor programs and as separate high resolution studies focused on detecting brown dwarf and planetary mass objects at wide separations, a large sample of stars have been observed with adaptive optics, coronagraphic instruments. Unfortunately, in most cases, only those stars with companion candidates or confirmed companions are published. As a result, there are numerous unpublished observations of potential targets resulting in repetitive observations of the same star in multiple studies. While these studies most likely have different inner working angles and overall sensitivities, there is value in having a public archive of previous observations to either weed out unknown, close stellar binaries or to facilitate the identification of common proper motion. In fact, it was archival images of HR 8799 from a previously unpublished AO survey of nearby stars that was used to detect the orbital motion of the directly imaged planets in this system (Marois et al. 2009). In addition, the absence of companions up to a given mass at a given separation for a large sample of stars can provide just as much information on planetary formation and dynamics as their detection. With this in mind, all of the AO images col-

lected for this survey will be donated to the NStED¹⁰ database and we encourage others to do the same.

7. CONCLUSIONS

We have completed a high contrast imaging survey of a sample of stars slated to be potential targets for the SIM Lite astrometric space telescope. While many of our observations were sensitive enough to detect brown dwarf companions at separations of $>1''$, our survey found two unpublished confirmed common proper motion stellar companions around GJ 454 and GJ 1020. This survey will serve as a resource for both SIM Lite and direct imaging surveys such as GPI and SPHERE as all the images will be given to the NStED database. These images can be used to vet future targets and aid in common proper motion determinations. Additional SIM-Lite targets will be observed with high contrast imaging if they have not

all ready been observed with other programs.

We would like to thank our anonymous referee for their valuable insights into how to improve our manuscript. We'd also like to thank Shri Kulkarni and Mike Shao for invaluable discussions regarding the selection of the EPICs targets. Based on observations obtained at the Hale Telescope, Palomar Observatory, as part of a continuing collaboration between the California Institute of Technology, NASA/JPL, and Cornell University. The research described in this publication was carried out at the Jet Propulsion Laboratory, California Institute of Technology, under a contract with the National Aeronautics and Space Administration. This publication makes use of data products from the Two Micron All Sky Survey, which is a joint project of the University of Massachusetts and the Infrared Processing and Analysis Center/California Institute of Technology, funded by the National Aeronautics and Space Administration and the National Science Foundation.

REFERENCES

- Baraffe, I., & Chabrier, G. 1996, ApJ, 461, L51
 Burrows, A., et al. 1997, ApJ, 491, 856
 Carson, J. C., Hiner, K. D., Villar, G. G., Blaschak, M. G., Rudolph, A. L., & Stapelfeldt, K. R. 2009, AJ, 137, 218
 Carson, J. E., et al. 2007, ApJ, 662, 199
 Catanzarite, J., Shao, M., Tanner, A., Unwin, S., & Yu, J. 2006, PASP, 118, 1319
 Cutri, R., et al., 2006, AJ, 31, 1163
 Golimowski, D. A., Henry, T. J., Krist, J. E., Schroeder, D. J., Marcy, G. W., Fischer, D. A., & Butler, R. P. 2000, AJ, 120, 2082
 Golimowski, D. A., Fastie, W. G., Schroeder, D. J., & Uomoto, A. 1995, ApJ, 452, L125
 Hartkopf, W. I., Mason, B. D., & McAlister, H. A. 1996, AJ, 111, 370
 Kalas, P., et al. 2008, Science, 322, 1345
 Lowrance, P. J., et al. 2005, AJ, 130, 1845
 Marois, C., Macintosh, B., Barman, T., Zuckerman, B., Song, I., Patience, J., Lafrenière, D., & Doyon, R. 2008, Science, 322, 1348
 McCarthy, C., & Zuckerman, B. 2004, AJ, 127, 2871
 Metchev, S. A., & Hillenbrand, L. A. 2009, ApJS, 181, 62
 Metchev, S., 2005, PhD Thesis, California Institute of Technology
 Metchev, S. A., & Hillenbrand, L. A. 2004, ApJ, 617, 1330
 Niedzielski, A., et al. 2007, ApJ, 669, 1354
 Tanner, A., et al. 2007, PASP, 119, 747
 Unwin, S. C., et al. 2008, PASP, 120, 38

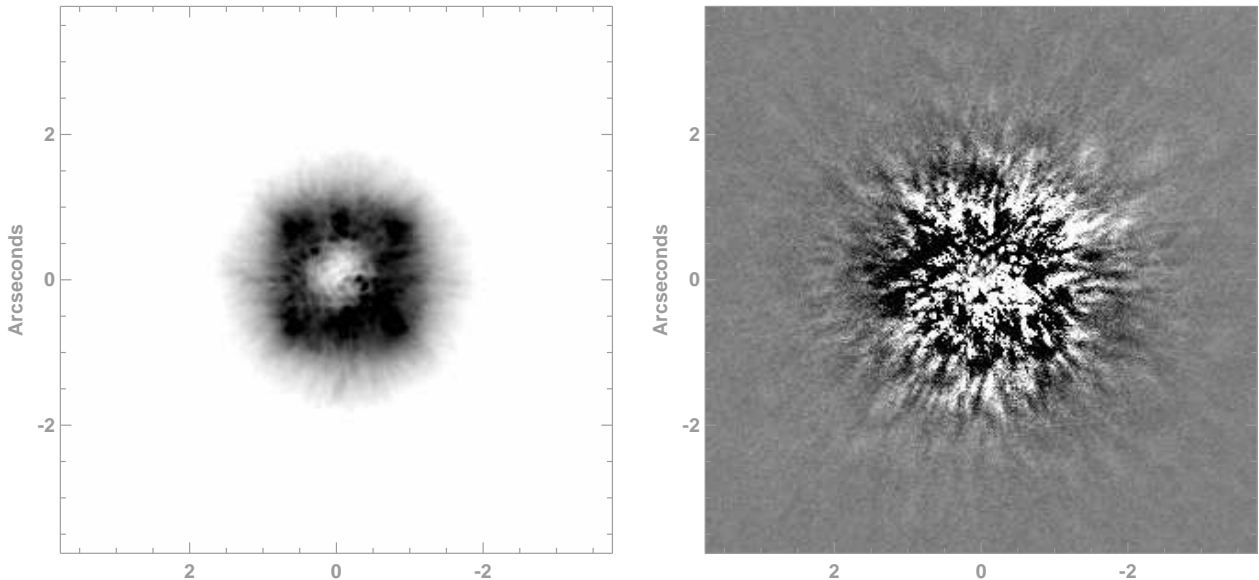


FIG. 1.— *Left* - Image of GL 876 prior to PSF subtraction. *Right* - The difference image between GL 876 and HD 216789 showing the reduced flux in the halo of the PSF as a result of the subtraction. North is up and East is to the left in all the images.

¹⁰ <http://nsted.ipac.caltech.edu>

TABLE 2
PALOMAR AO SAMPLE - CONT.

| Target | RA | Dec | μ_α mas/yr | μ_δ mas/yr | V | Ks | SpTy | Distance pc | Observing Dates | t_{int} sec |
|------------|-------------|--------------|------------------------|------------------------|-------|------|------|----------------|---------------------|------------------|
| GJ 820 A | 21 06 53.94 | +38 44 57.90 | 4157 | 3259 | 5.21 | 2.25 | K5V | 3.48 | June 2004; Nov 2005 | 5.4 |
| GJ 820 B | 21 06 55.26 | +38 44 31.40 | 4109 | 3144 | 6.03 | 2.54 | K7V | 3.50 | June 2004; Nov 2005 | 5.4 |
| GJ 821 | 21 09 17.42 | -13 18 09.02 | 710 | -1995 | 10.87 | ... | M1 | 12.15 | June 2004; Nov 2005 | 270 |
| GJ 848.4 A | 22 09 29.87 | -07 32 55.16 | 85 | -450 | 6.63 | 4.89 | G0V | 21.29 | June 2004 | 270 |
| GJ 849 | 22 09 40.35 | -04 38 26.62 | 1135 | -20 | 10.42 | 5.59 | M3.5 | 8.77 | Aug 2004 | 500 |
| GJ 872 A | 22 46 41.58 | +12 10 22.40 | 233 | -492 | 4.20 | 2.96 | F7V | 16.25 | June 2005 | 60 |
| GJ 873 | 22 46 49.73 | +44 20 02.37 | -705 | -459 | 10.09 | 5.30 | M3.5 | 5.05 | June 2004; Nov 2005 | 10; 600 |
| GJ 875 | 22 50 19.43 | -07 05 24.39 | -103 | 103 | 9.97 | 6.10 | K7 | 14.00 | Oct 2004 | 1800 |
| GJ 876 | 22 53 16.73 | -14 15 49.32 | 960 | -676 | 10.17 | ... | M4 | 4.70 | July 2004 | 650 |
| GJ 882 | 22 57 27.98 | +20 46 07.80 | 208 | 61 | 5.49 | 3.91 | G5V | 15.36 | June 2005 | 180 |
| GJ 884 | 23 00 16.12 | -22 31 27.65 | -904 | 58 | 7.89 | 4.48 | K5V | 8.14 | July 2004 | 450 |
| GJ 889 A | 23 07 07.06 | -23 09 34.01 | 154 | -254 | 9.61 | 6.42 | K6V | 21.11 | July 2004 | 650 |
| GJ 892 | 23 13 16.98 | +57 10 06.08 | 2075 | 295 | 5.56 | 3.26 | K3V | 6.53 | June 2004 | 5.4 |
| GJ 898 | 23 32 49.40 | -16 50 44.31 | 344 | -218 | 8.60 | 5.47 | K6Vk | 13.95 | July 2004 | 900 |

TABLE 3
TABLE OF OBSERVATIONS

| Date | Seeing Conditions ["] ^a |
|------------------|------------------------------------|
| 1-3 June 2004 | 0.5 |
| 1-3 Aug 2004 | 1.0 |
| 6-7 Oct 2004 | 0.5 |
| 11 - 14 Nov 2004 | 0.7 |
| 31 Dec 2004 | 2.0 |
| 7 Jul 2005 | 1.5 |
| 12-14 Nov 2005 | 0.7 |
| 7 Dec 2005 | 3.0 |

^a Seeing is estimated from the FWHM of one of the target stars observed with the adaptive optics turned off.

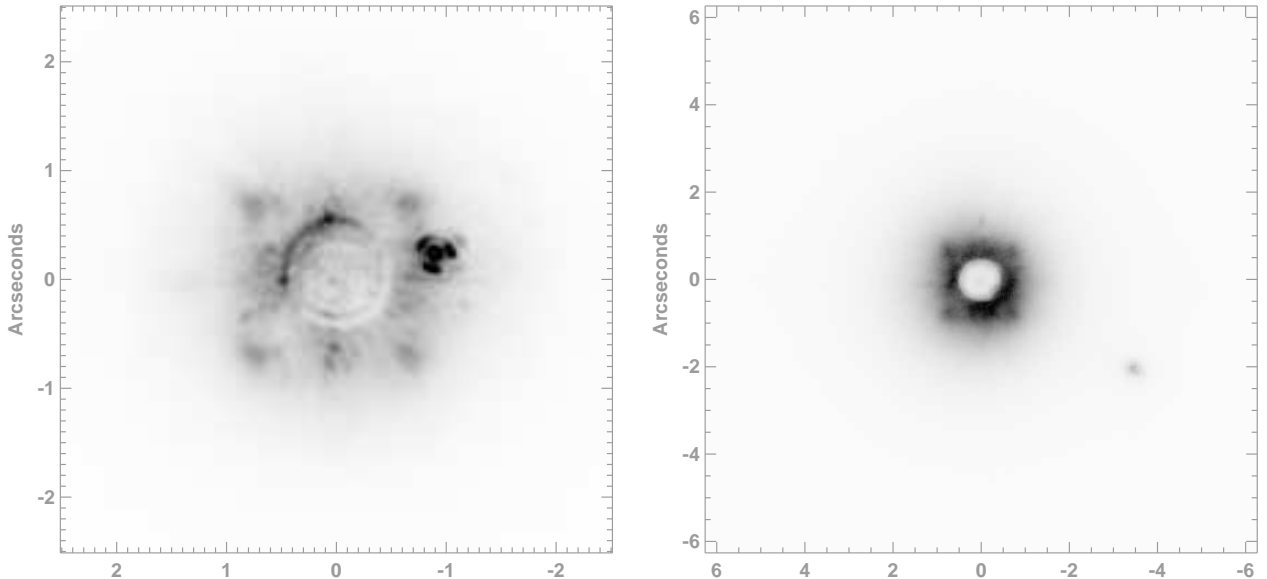


FIG. 2.— *Left* - Image of GL 454 and its common proper motion companion with a K_s magnitude of 7.75 and a separation of $0.95''$. *Right* - Image of GL 1020 with a $K_s=10.34$ magnitude companion $4''$ away.

TABLE 4
STARS WITH NO COMPANION CANDIDATES IN THE FIELD OF VIEW

| | |
|----------|----------|
| GJ 10 | GJ 628 |
| GJ 34 A | GJ 629.1 |
| GJ 34 B | GJ 663 A |
| GJ 37 | GJ 663 B |
| GJ 61 A | GJ 664 |
| GJ 68 | GJ 670 B |
| GJ 71 | GJ 678 A |
| GJ 79 | GJ 687 |
| GJ 107 A | GJ 692 |
| GJ 111 | GJ 699 |
| GJ 137 | GJ 702 B |
| GJ 147 | GJ 725 A |
| GJ 167 | GJ 725 B |
| GJ 204 | GJ 768 |
| GJ 303 | GJ 785 |
| GJ 338 A | GJ 796 |
| GJ 382 | GJ 805 |
| GJ 394 | GJ 811 |
| GJ 423.1 | GJ 820 A |
| GJ 447 | GJ 821 |
| GJ 448 | GJ 849 |
| GJ 506 | GJ 872 A |
| GJ 526 | GJ 875 |
| GJ 527 A | GJ 876 |
| GJ 555 | GJ 882 |
| GJ 557 | GJ 884 |
| GJ 570 A | GJ 889 A |
| GJ 581 | GJ 898 |
| GJ 598 | GJ 3175 |
| GJ 602 | GJ 4324 |
| GJ 606.2 | GJ 9207 |
| GJ 616 | GJ 9491 |

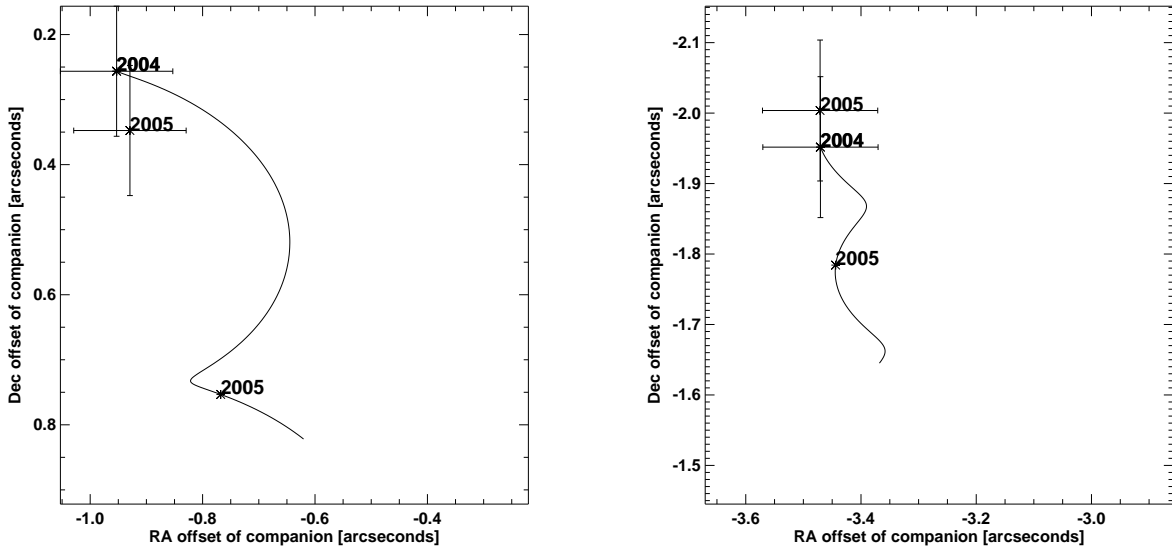


FIG. 3.— Plots of the offsets in RA and Dec for the companion candidates around GL 454 and GL 1020. The squiggly line denotes the expected change in the offset if the companion were a background object. The labels (i.e. 2004, 2005) indicate the epochs of the observed offsets and the expected offsets of a background object at the epochs of the observations. The fact that the observed offsets are consistent with each other within the uncertainties suggests these two companions are bound to the star.

TABLE 5
COMPANION CANDIDATES

| Target | K_{target}^a | Separation " | PA deg | K_{scomp} | Epoch | Status ^b |
|---------------------|-----------------------|------------------|------------|--------------------|-----------|---------------------|
| GJ 15 A | 4.02±0.02 | 6.40±0.12 | 158.3±3.2 | 15.98±0.06 | Oct 2004 | NCPM |
| GJ 15 B | 5.95±0.02 | 7.54±0.12 | 66.2±0.4 | 16.52±0.06 | Oct 2004 | NCPM |
| | | 11.91±0.14 | 70.3±0.3 | 16.20±0.06 | Oct 2004 | NCPM |
| GJ 72 | 4.60±0.02 | 9.93±0.12 | -79.4±0.4 | 11.85±0.06 | Aug 2004 | NCPM |
| GJ 105 A | 3.48±0.21 | 2.63±0.12 | -54±0.2 | 8.77±0.22 | Aug 2004 | CPM ^c |
| GJ 107 B | 5.87±0.02 | 6.24 μ m0.12 | 161.3±4.3 | 17.70±0.06 | Oct 2004 | U |
| GJ 115 A | 6.70±0.02 | 6.50±0.12 | 156.2±2.5 | 18.81±0.06 | Aug 2004 | U |
| GJ 250 B | 5.72±0.04 | 9.62±0.13 | -27.2±1.4 | 14.04±0.07 | Nov 2005 | U |
| GJ 302 | 4.17±0.04 | 9.99±0.13 | -152.5±1.3 | 15.46±0.07 | Dec 2004 | NCPM |
| GJ 454 | 4.03±0.26 | 0.99±0.12 | -75.5±03.2 | 7.75±0.06 | July 2005 | CPM |
| GJ 670 A | 3.07±0.30 | 10.79±0.14 | -98.9±0.4 | 13.74±0.38 | June 2004 | U |
| GJ 701 | 5.31±0.02 | 12.36±0.13 | 136.2±0.3 | ... | Aug 2004 | NCPM |
| GJ 702 AB | 1.79±0.30 | 9.38±0.13 | -128.9±0.3 | 13.01±0.30 | Aug 2004 | U |
| | | 11.53±0.14 | -164.5±0.3 | 13.82±0.30 | Aug 2004 | U |
| GJ 716 | 4.70±0.02 | 2.84±0.12 | 170.0±3.2 | 14.06±0.06 | Aug 2004 | NCPM |
| | | 3.54±0.13 | -92.8±0.9 | 15.72±0.06 | Aug 2004 | NCPM |
| | | 5.11±0.13 | -147.4±1.4 | 15.75±0.06 | Aug 2004 | NCPM |
| | | 5.30±0.14 | 71.2±1.2 | 15.91±0.06 | Aug 2004 | NCPM |
| | | 5.38±0.13 | 119.0±1.6 | 13.62±0.06 | Aug 2004 | NCPM |
| GJ 722 ^d | 4.23±0.02 | 5.02±0.12 | -20.2±5.4 | 15.90±0.06 | Aug 2004 | NCPM |
| | | 6.40±0.12 | 30.1±1.5 | 17.50±0.06 | Aug 2004 | NCPM |
| GJ 726 ^d | 5.58±0.03 | 2.11±0.12 | -93.6±1.5 | 13.63±0.06 | June 2004 | U |
| | | 2.46±0.12 | -136.0±1.4 | 14.31±0.06 | June 2004 | U |
| | | 3.09±0.12 | -122.7±1.0 | 17.62±0.06 | June 2004 | U |
| | | 3.85±0.12 | -4.8±1.2 | 16.42±0.06 | June 2004 | U |
| GJ 729 | 5.37±0.02 | 6.24±0.12 | -49±0.5 | 17.04±0.06 | Aug 2004 | U |
| | | 8.34±0.13 | -126.0±0.4 | 17.70±0.06 | Aug 2004 | NCPM |
| GJ 779 | 4.39±0.03 | 3.30±0.12 | -77.5±0.9 | 13.53±0.06 | Aug 2004 | NCPM |
| | | 6.21±0.12 | 162.0±5.2 | 12.38±0.06 | Aug 2004 | NCPM |
| | | 9.34±0.13 | 140.1±0.9 | 12.97±0.06 | Aug 2004 | NCPM |
| GJ 789 | 4.90±0.02 | 12.78±0.14 | 67.9±0.3 | 15.41±0.06 | Aug 2004 | U |
| GJ 820 B | 2.54±0.33 | 11.51±0.14 | 77.4±0.4 | 14.8±0.06 | Nov 2005 | U |
| GJ 848.4 | 4.60±0.02 | 6.69±0.12 | -158.2±3.1 | 16.5±0.06 | June 2004 | U |
| GJ 873 | 5.30±0.02 | 6.47±0.12 | 175.5±3.0 | ... | Nov 2005 | U |
| | | 5.78±0.12 | 115.6±0.2 | ... | Nov 2005 | U |
| GJ 892 | 3.26±0.30 | 6.99±0.12 | 44.5±0.5 | ... | June 2004 | NCPM |
| | | 9.93±0.13 | -17.9±0.9 | ... | June 2004 | U |
| | | 11.14±0.12 | -74.4±0.8 | ... | June 2004 | U |
| GJ 1020 | 4.62±0.02 | 3.98±0.12 | -119.4±0.7 | 10.34±0.06 | Dec 2004 | CPM |

^a K_s magnitudes and errors taken from the 2MASS catalog (Cutri et al. 2006).

^b NCPM= non-common proper motion, CPM=common proper motion, U=unconfirmed

^c Companion around GJ 105a was originally identified by Golimowski et al. 1995

^d Star in crowded field. Not all companions in the field of view are listed.

TABLE 6
ASTROMETRY FOR CONFIRMED COMPANIONS

| Target | ρ ["] | PA [deg] | Epoch |
|---------|-------------|--------------|-------------|
| GL 454 | 0.987±0.115 | -75.06±3.23 | June 4 2004 |
| | 0.992±0.115 | -75.51±3.12 | July 7 2005 |
| GL 1020 | 3.98±0.12 | -119.35±0.74 | Dec 31 2004 |
| | 4.01±0.12 | -119.97±0.74 | Nov 14 2005 |

TABLE 7
PALOMAR IMAGING SENSITIVITIES, ΔK_S AT 90% COMPLETENESS

| Target | 0.5" | 1" | 2" | 5" |
|----------|------|------|-------|-------|
| GJ 10 | 6.32 | 6.54 | 7.91 | 10.20 |
| GJ 1020 | 6.08 | 6.01 | 7.16 | 9.30 |
| GJ 105a | 5.82 | 5.93 | 7.25 | 9.29 |
| GJ 107a | 6.04 | 6.18 | 7.61 | 10.43 |
| GJ 107b | 7.52 | 8.33 | 10.21 | 12.77 |
| GJ 111 | 6.31 | 6.44 | 8.02 | 9.74 |
| GJ 115a | 9.67 | 9.92 | 11.66 | 13.46 |
| GJ 137 | 5.45 | 5.70 | 7.04 | 8.96 |
| GJ 147 | 5.73 | 6.01 | 7.56 | 10.24 |
| GJ 15a | 6.61 | 6.95 | 7.99 | 10.24 |
| GJ 15b | 8.00 | 8.26 | 9.55 | 12.22 |
| GJ 204 | 6.95 | 7.17 | 8.44 | 10.30 |
| GJ 303 | 6.54 | 6.97 | 8.36 | 10.54 |
| GJ 3175 | 6.86 | 6.98 | 8.48 | 10.20 |
| GJ 37 | 6.16 | 6.25 | 8.06 | 9.95 |
| GJ 454 | 5.56 | 5.79 | 7.35 | 8.45 |
| GJ 506 | 5.24 | 5.36 | 6.23 | 8.54 |
| GJ 527a | 6.37 | 6.10 | 7.51 | 9.37 |
| GJ 602 | 4.55 | 4.82 | 5.78 | 7.26 |
| GJ 606.2 | 5.62 | 5.40 | 7.15 | 8.76 |
| GJ 616 | 5.91 | 5.88 | 7.55 | 8.25 |
| GJ 61a | 7.60 | 8.25 | 9.75 | 12.21 |
| GJ 629.1 | 9.56 | 8.64 | 10.02 | 10.93 |
| GJ 68 | 6.04 | 6.33 | 7.83 | 9.79 |
| GJ 699 | 6.19 | 6.54 | 8.60 | 11.08 |
| GJ 702a | 4.34 | 4.87 | 6.25 | 8.97 |
| GJ 71 | 7.81 | 4.73 | 5.43 | 8.50 |
| GJ 725b | 6.57 | 6.94 | 8.08 | 9.72 |
| GJ 729 | 7.51 | 7.72 | 8.79 | 9.97 |
| GJ 779 | 6.98 | 6.97 | 8.81 | 10.38 |
| GJ 785 | 5.98 | 6.19 | 7.64 | 10.29 |
| GJ 789 | 7.31 | 7.57 | 6.84 | 9.18 |
| GJ 805 | 5.70 | 5.72 | 6.84 | 9.18 |
| GJ 811 | 6.62 | 6.61 | 7.51 | 9.25 |
| GJ 820a | 3.67 | 3.95 | 4.94 | 7.36 |
| GJ 820b | 4.44 | 4.54 | 5.75 | 7.78 |
| GJ 849 | 7.84 | 8.11 | 9.70 | 12.00 |
| GJ 872a | 5.67 | 5.71 | 7.43 | 9.15 |
| GJ 873 | 7.68 | 7.99 | 8.96 | 11.07 |
| GJ 882 | 6.32 | 6.21 | 8.12 | 9.90 |
| GJ 884 | 7.45 | 7.66 | 8.95 | 11.14 |
| GJ 889a | 8.18 | 7.92 | 9.05 | 9.45 |
| GJ 898 | 9.54 | 9.91 | 10.00 | 12.35 |
| GJ 9491 | 6.20 | 6.28 | 7.73 | 10.82 |

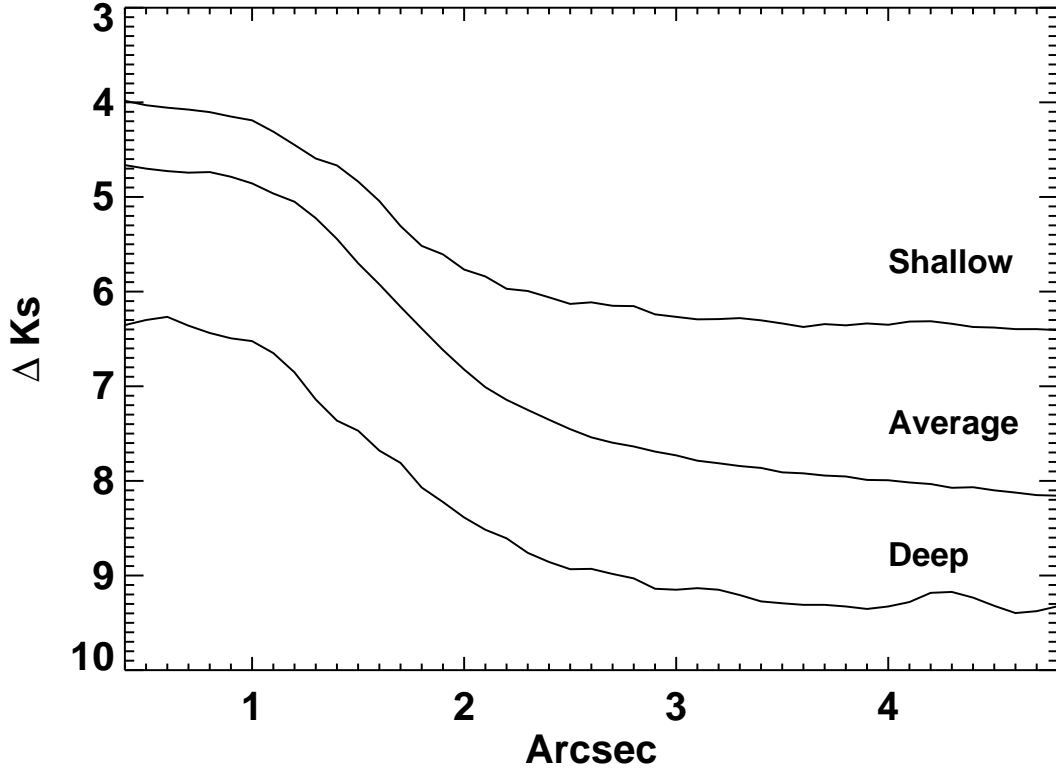


FIG. 4.— Plot of the differential magnitude detectable in the PHARO images as a function of distance from the star in arcseconds. The three lines represent the averages of three levels of sensitivity which corresponds to values at $3''$ of $\Delta K_s > 6$, $5 < \Delta K_s < 4$, and $\Delta K_s < 4$ magnitudes, respectively. The sensitivity of any image depends both on the integration time of the exposure and the seeing conditions.

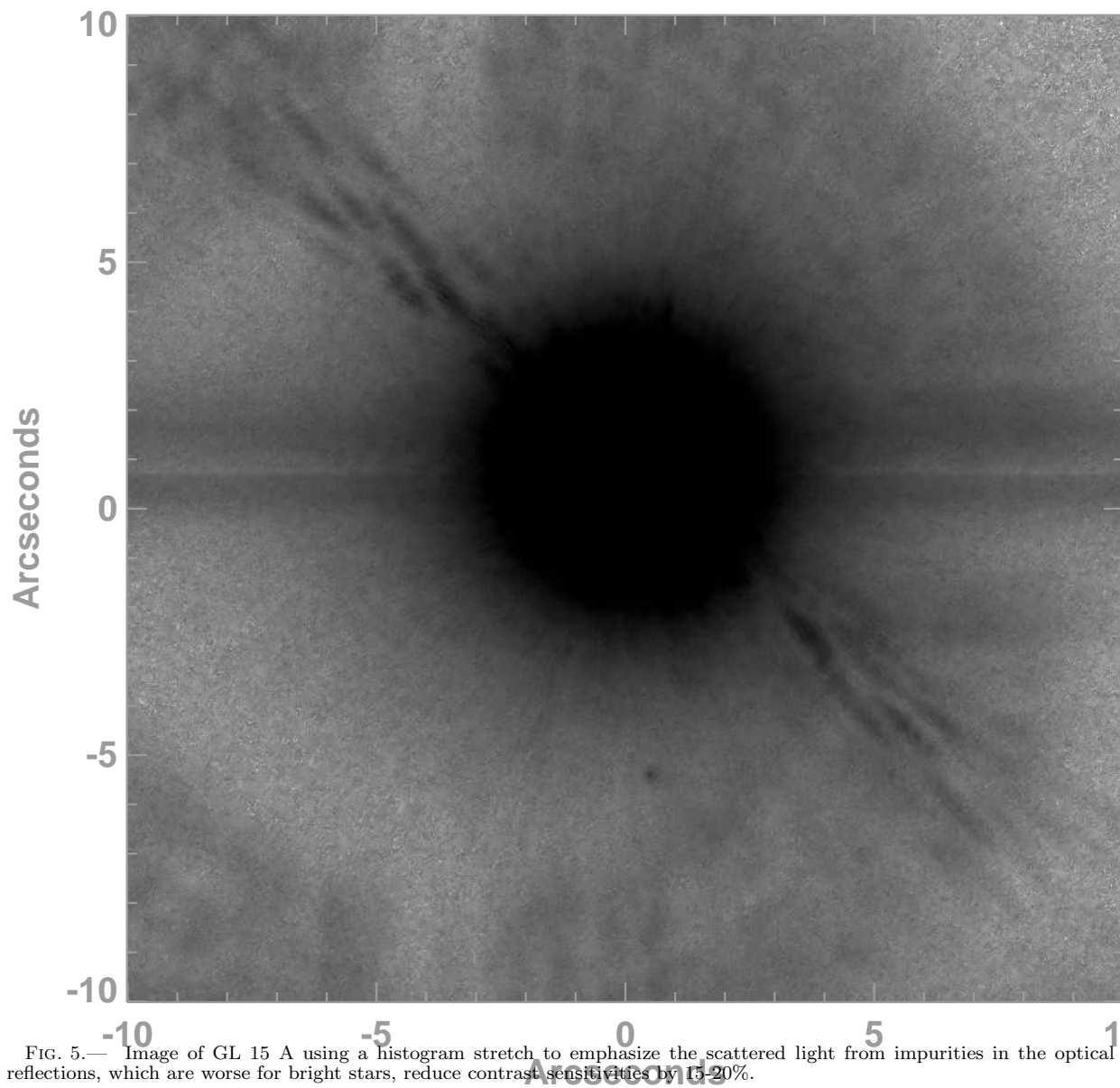


FIG. 5.— Image of GL 15 A using a histogram stretch to emphasize the scattered light from impurities in the optical path. These reflections, which are worse for bright stars, reduce contrast sensitivities by 15-20%.

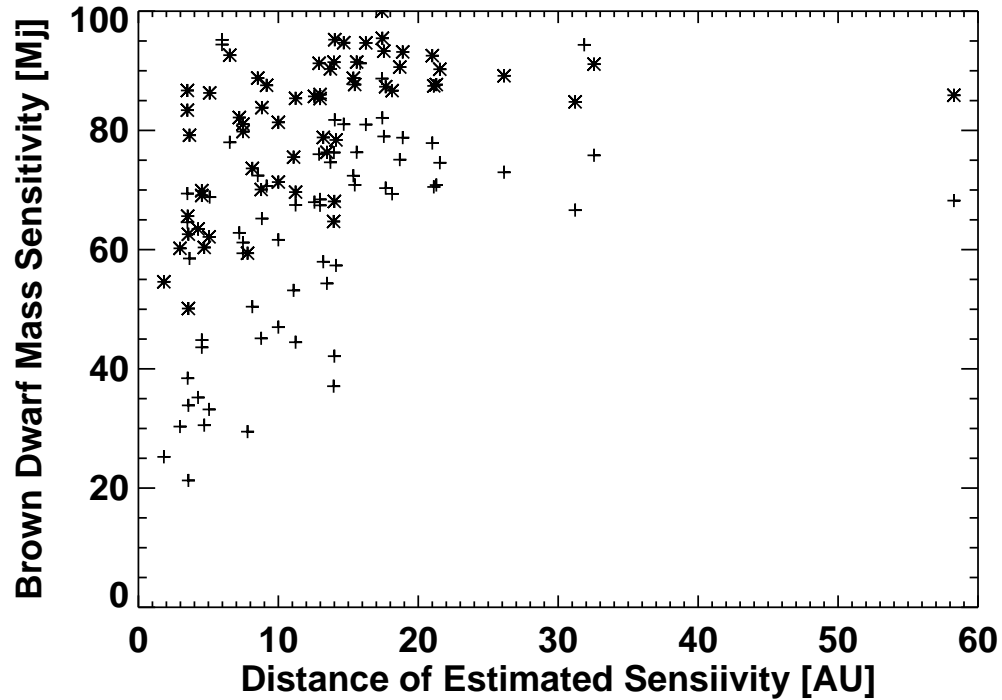


FIG. 6.— Minimum companion mass limits (Burrows et al. 1997) estimated from PSF planting as a function of projected physical distance from the star assuming ages of both 1 Gyr (+) and 5 Gyr (*). We are sensitive to brown dwarf mass companions ($M < 75 M_J$) for many of the stars in the survey.

FIG. 7.— Images of the SIM Lite target stars with unidentified or confirmed background stars in their $25''$ field-of-view. We have circled some of the stars to aid the reader. (These figures are available upon request.)